

International Journal of Hydrology Science and Technology

ISSN online: 2042-7816 - ISSN print: 2042-7808

<https://www.inderscience.com/ijhst>

Conjunctive use of flow modelling, entropy, and GIS to design the groundwater monitoring network in the complex aquifer system

Yashwant B. Katpatal, Chandan Kumar Singh

DOI: [10.1504/IJHST.2021.10041387](https://doi.org/10.1504/IJHST.2021.10041387)

Article History:

Received:	09 December 2020
Accepted:	31 May 2021
Published online:	21 December 2022

Conjunctive use of flow modelling, entropy, and GIS to design the groundwater monitoring network in the complex aquifer system

Yashwant B. Katpatal

Department of Civil Engineering,
Visvesvaraya National Institute of Technology,
Nagpur, India
Email: ybkatpatal@rediffmail.com

Chandan Kumar Singh*

Department of Civil Engineering,
National Institute of Technology,
Raipur, India
Email: cksingh.ce@nitrr.ac.in
*Corresponding author

Abstract: The groundwater level monitoring network (GWLMN) provides a basis for management and planning of groundwater resources. The present study aims to assess and redesign the GWLMN for the Wainganga Basin, Central India. The study proposes a three-step method to redesign the GWLMN: 1) to simulate spatiotemporal distribution of groundwater levels (GWLs) using groundwater flow modelling (GWFM); 2) to analyse the uncertainty in GWL for each observation wells (OWs) using entropy theory; 3) to optimise GWLMN using hydrological and anthropogenic parameters. The study suggests that, a minimum of 116 OWs were significant for GWLMN. Incorporation of hydrological and anthropogenic parameters into the GIS environment is found to be important for designing GWLMN. The proposed method is useful for redesigning GWLMN in a complex aquifer system.

Keywords: groundwater monitoring; geographic information systems; entropy; MODFLOW; monitoring network; observation well.

Reference to this paper should be made as follows: Katpatal, Y.B. and Singh, C.K. (2023) 'Conjunctive use of flow modelling, entropy, and GIS to design the groundwater monitoring network in the complex aquifer system', *Int. J. Hydrology Science and Technology*, Vol. 15, No. 1, pp.78–96.

Biographical notes: Yashwant B. Katpatal is currently a Professor at the Department of Civil Engineering, Visvesvaraya National Institute of Technology, Nagpur, India. He has vast 28 years of teaching and research experience. He supervised 22 PhDs and over 100 UG and PG students. His research interests include hydrogeology, climate change, groundwater hydrology, water resource management, environmental impact assessment, remote sensing and geographic information systems. He served on several administrative responsibilities including the Associate Dean of International Affairs, the Chairman of Special Cell of VNIT, member of APEC, a convener in Institute of Eminence, the Chairman in the International Affairs Committee, etc.

Chandan Kumar Singh is currently an Assistant Professor at the Department of Civil Engineering, National Institute of Technology, Raipur, India. He worked as a Postdoctoral Scholar in the Sierra Nevada Research Institute at the University of California, Merced, USA. He received his PhD from the Department of Civil Engineering in the Visvesvaraya National Institute of Technology, Nagpur, India in 2018. His research interests are geo-informatics application in groundwater management, water resource management, watershed and regional scale hydrologic modelling, climate change impact and adaptation.

1 Introduction

Evaluation of the groundwater resources and understanding of the complex hydrogeologic process is essential for planning, designing, and management of groundwater resources (Varalakshmi et al., 2014). Groundwater level (GWL) monitoring using observation wells (OWs) is one of the essential parts of groundwater management. The purpose of a groundwater level monitoring network (GWLMN) is to enhance the understanding of the hydrogeologic system through the systematic collection of GWL data (Hosseini and Kerachian, 2017). OWs are used for long-term and systematic monitoring of groundwater quality and quantity within space and time. Improper spatial and temporal distribution of OWs in complex aquifer systems may return unrepresentative information about the groundwater resources. In a complex aquifer system, arid and semiarid climatic conditions, and increased exploitation of groundwater may make the monitoring system highly uncertain (Singh and Katpatal, 2017a). It is not feasible to add OWs at every location, but it is essential to know the status of groundwater at unmonitored locations. Hence, a redesign of an optimised network of GWL is significant for an effective groundwater management.

In recent studies, various authors have applied different approaches to the design of hydrometric networks such as precipitation and GWLMNs (Mishra and Coulibaly, 2009; Wang et al., 2017). Some authors state that the geostatistical-based approach is an effective method to reduce the interpolation discrepancy of the monitoring network (Júnez-Ferreira and Herrera, 2013; Ritzi and Soltanian, 2015; Singh and Katpatal, 2017b). In addition, statistical and entropy theory-based methods have been extensively used in the design of GWLMN (Singh and Katpatal, 2020a). In general, the hydrometric monitoring networks have been optimised to achieve a systematic and long-term data collection by increasing the accuracy and reducing the uncertainty (Li et al., 2012). Mondal and Singh (2012) have employed the discrete-based entropy theory to evaluate GWLMN. Hosseini and Kerachian (2017) have considered a different approach with entropy theory to redesign the groundwater monitoring network. Also, many authors have analysed and studied groundwater flow models for different purposes, such as to predict (deterministic) or forecast (probabilistic) the aquifer response under anthropogenic changes (Mondal et al., 2011; Katpatal et al., 2014; Varalakshmi et al., 2014), to simulate the aquifer system (Ansari et al., 2016), and to generate the hypothetical system to study the principles of groundwater flow system (Shigidi and Garcia, 2003). The numerical-based groundwater model simulates the complex hydrological process using a set of governing equations (Todd and Mays, 1980). The groundwater flow model can

provide the solution on the continuous spatial domain. To date, no study has been found to optimise the GWLMN using groundwater modelling.

In the aforementioned studies, the geostatistical-based optimisation method mainly focuses on the statistical relationship within hydrometric networks. In addition, entropy theory has been used extensively in different hydrological applications (Singh and Katpatal, 2020b). However, less consideration has been given to the spatiotemporal distribution and hydrological characteristics of the hydrometric network. The complexity of the aquifers has a measurable impact on the groundwater availability and movement (Kelly et al., 2013). Yet, less attention has been given to redesigning of GWLMN in complex aquifer systems.

To overcome the aforementioned limitations, the present study demonstrates a simple and new optimisation technique to redesign the GWLMN in the Wainganga Basin, Central India. This study utilises entropy-based theory and groundwater flow model (MODFLOW) in a GIS environment to optimise the GWLMN. The advantage of applying the groundwater model is that it provides continuous GWL data in the spatial and temporal domain, whereas entropy theory analyses only discrete field data. Hence, a combination of the groundwater flow model and entropy theory in GIS environment has been proposed to redesign the network that incorporates the continuous spatial phenomenon, spatial uncertainty and hydrological and anthropogenic factors. This paper is organised as follows: the methods used to optimise the GWL monitoring network which is described concisely in the materials and methods section, the hypothetically assumed network of OWs, the output obtained from the groundwater flow modelling, the uncertainty analysis using entropy theory and used to redesign the GWL network given in the results and discussion section. The major findings from the study are presented as conclusions.

2 Materials and methods

In this section, three steps were proposed to redesign the GWLMN in the complex aquifer system of the Wainganga Sub-Basin. The first step aims to simulate groundwater model of the study area under steady state condition using MODFLOW. The second step includes the application of entropy theory to evaluate the uncertainty in each OW with the change in season from the year 1999 to 2012. The third step demonstrates the application of GIS, groundwater flow model and uncertainty analysis to optimise the GWLMN in irrigated regions of the complex aquifer system. The overall methodology and the hydrological factors applied in the present study are explained in Figure 1.

2.1 Study area

The Wainganga Sub-Basin is located between $20^{\circ}35' - 21^{\circ}44'N$ and $78^{\circ}15' - 79^{\circ}40'E$ in Central India (Figure 2). The altitude of the study area varies between 119 and 527 m above mean sea level (amsl). The study area covers 3,320 km². The average annual precipitation in the study area is about 800 to 1,200 mm (Chandan and Yashwant, 2017). The study area comprises six complex aquifer systems, namely alluvium, amgaon gneissic complex, mica schist, basalt, calc gneiss marble, and an unclassified gneissic complex (GSI, 2009; Manzar, 2013) (Figure 1 and Table 1). Kanhan is the major river flowing through the middle of the study area. Depending upon the source of water

supply, the study area is classified as command area (CA) and non-command area (NCA). Groundwater is the major source of water supply in the NCA while, surface water is a major source of water supply in the CA (CWC and NRSC, 2014). The groundwater resource available in the study area is 170–200 MCM/year (Singh and Katpatal, 2017b). The existing GWLMN in the region consists of 30 OWs. The continuous GWLs measurement in January, March, May and October months was recorded from the year 1999 to 2012 (CGWB, 2012, 2014).

Figure 1 Flow chart showing the overall method (see online version for colours)

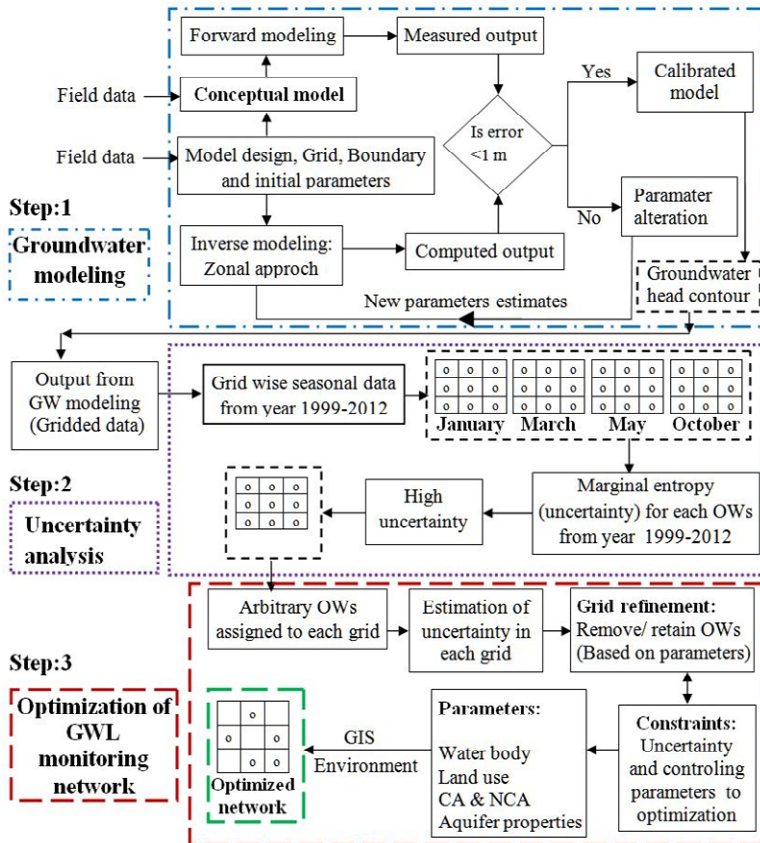
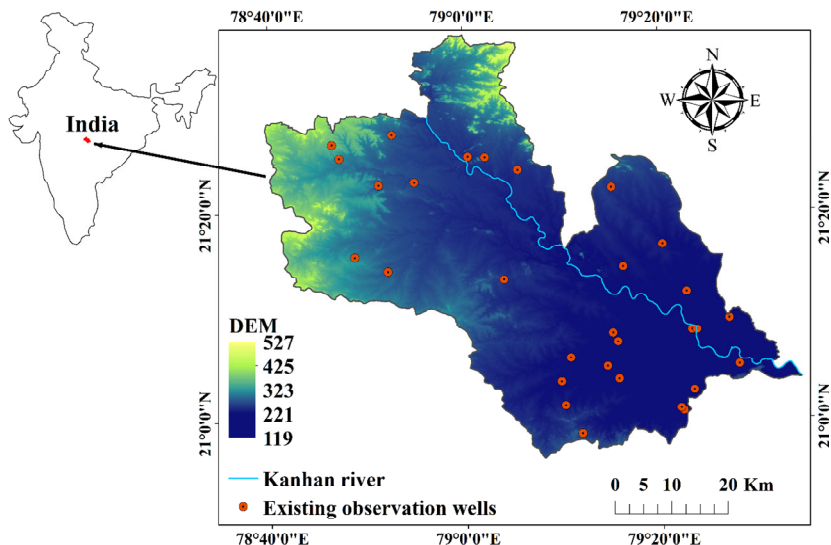


Table 1 Aquifer system of the study area

Sr. no.	Aquifer	Yield (m ³ /day)	Specific yield (%)
1	Basalt	13–56	2–3.5
2	Amgaon Gneissic Complex	10–33	Up to 1.5
3	Alluvium	70–350	6–10
4	Unclassified Gneiss Tirodi Gneissic Complex	10–35	Up to 1.5
5	Calc Gneiss and Marble	18–36	1.5–2
6	Mica Schist	18–27	1.5–2

Figure 2 Location map of the study area representing digital elevation model (DEM), river and existing OWs (see online version for colours)

2.2 Groundwater flow modelling

2.2.1 Conceptual model

The study area comprises complex aquifer formations. Based on the hydrogeology of the study area, a single layer unconfined aquifer was conceptualised with an average thickness of 30 m. The details of the complex aquifer system are shown in Table 1. The groundwater flow model of the study area was simulated using Groundwater Modelling System (GMS) software 7.1. An unconfined, anisotropic and heterogeneous aquifer was assumed to model the 2D groundwater flow (steady state) in the Wainganga Sub-Basin [equation (1)].

$$\frac{\partial}{\partial x} \left(K_x h \frac{\partial h}{\partial x} \right) + \frac{\partial}{\partial y} \left(K_y h \frac{\partial h}{\partial y} \right) = 0 \quad (1)$$

Directional components of hydraulic conductivity (m/day), h = head (m).

A ‘conceptual model approach’ was used in which, raster layers in the map module of GMS software were used to prepare a conceptual model of the study area. All the necessary input data and parameters such as OWs, river/drainage, top and bottom elevation of the aquifer, hydraulic conductivity, recharge, starting head, etc. were created as raster layers and defined at the conceptual model level. Subsequently, the 2D grid was created and the conceptual model was changed to the grid-based MODFLOW numerical model and cell to cell computations were performed.

2.2.2 Model design

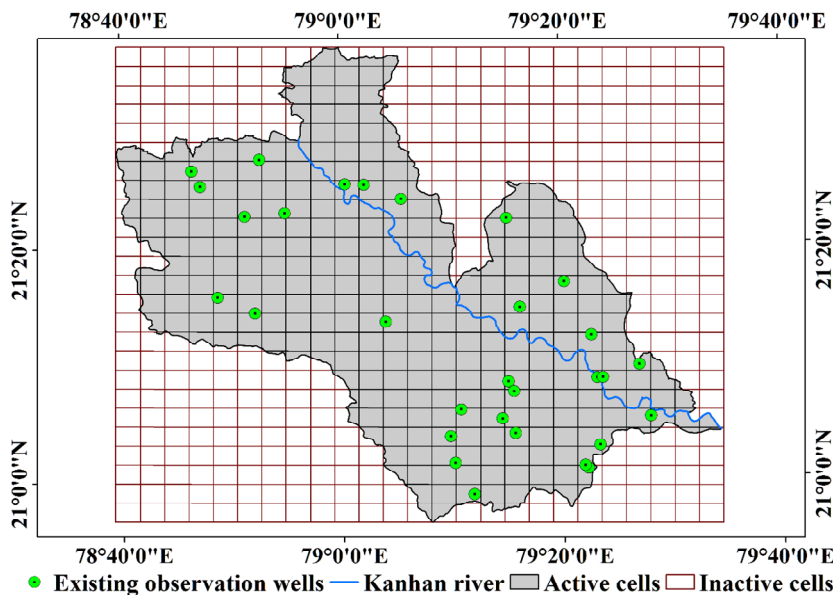
For the model, a domain of 95.65 km by 75.31 km was considered and discretised into 625 cells (25 columns and 25 rows) with cell dimension of 3 km by 3.8 km each

(Figure 3). The cells outside the boundary of the study area were marked as inactive cells. The study area was discretised into 310 active cells and 315 inactive cells. The aquifer condition of May 2011 was assumed to be the initial condition for the model calibration. The water level data for May (pre-monsoon) 2011 was interpolated using the simple kriging method (Davis, 2002) and the resulting interpolated data was exported to GMS MODFLOW, as the initial head (input) for groundwater flow simulation.

2.2.3 Model calibration

The model was run for the steady flow rate and groundwater contours were created by the model. Several trials and error were executed to calibrate the hydraulic conductivity. Parameters such as hydraulic conductivity were adjusted, and the model was iteratively run until the computed value matched measured output values (field observation) within a calibration target. The calibration target value of the water level of ± 1 m was defined. Initially, a forward model was run to calibrate the model within an acceptable level of accuracy. But after running the model for several trials, the set calibration target was not achieved by the forward model. Subsequently, an inverse modelling (zonal approach) was performed to calibrate the model. In this approach, the model was initialised by adding starting groundwater head values (field observation) and then trial hydraulic parameter values were added. The inverse model was run to adjust the trial parameter values till the calibration was reached. The field values were then exported for each grid for years 1999 to 2012 for January, March, May and October.

Figure 3 Model boundary with active and inactive cells (see online version for colours)



2.3 Uncertainty analysis

Groundwater head ('m' amsl) contours obtained from the groundwater flow modelling were used for uncertainty analysis. The results obtained from the flow modelling were

exported as a grid of size 3 km × 3.8 km. A hypothetical network was assumed to add OW in each grid for which, a hypothetical monitoring network of 310 OWs was assumed. The uncertainty in each OWs was estimated using entropy theory during 1999 to 2012 in January, March, May and October months [equation (2)]. Shannon coined the concept of entropy theory to measure the uncertainty in the random variables (Shannon and Weaver, 1949). The marginal entropy (ME) of the random variables X (GWLs in each OWs) with N (310 OWs) number of events is expressed as:

$$H(X) = - \sum_{n=1}^N p(x_n) \log_2 p(x_n) \quad (2)$$

where $H(X)$ is the ME of X random variables and $p(x)$ is the marginal probability distribution and $n = 1, 2, 3, \dots, N$. For the computation of ME [equation (2)], log base 2 was used and for a log base 2, the unit is ‘bit’ (Samuel et al., 2013). The ME represents the uncertainty in the random variable X . An increase in ME values is related to loss in information and decrease in the entropy values indicates a gain in information.

Table 2 Selected frequency class for computation of ME

<i>Frequency class</i>	<i>GWL range</i>	<i>Frequency class</i>	<i>GWL range</i>
1	<200	23	305–310
2	200–205	24	310–315
3	205–210	25	315–320
4	210–215	26	320–325
5	215–220	27	325–330
6	220–225	28	330–335
7	225–230	29	335–340
8	230–235	30	340–345
9	235–240	31	345–350
10	240–245	32	350–355
11	245–250	33	355–360
12	250–255	34	360–365
13	255–260	35	365–370
14	260–265	36	370–375
15	265–270	37	375–380
16	270–275	38	380–385
17	275–280	39	385–390
18	280–285	40	390–395
19	285–290	41	395–400
20	290–295	42	400–405
21	295–300	43	405–410
22	300–305	44	>410

The assumed hypothetical monitoring network has continuous GWLs data for the 14 year period (1999–2012) with 17,360 observations for January, March, May and October. All

GWL observations obtained from the groundwater flow model were classified in 44 class intervals ranging from 200 to 410 m amsl (Table 2). A frequency table was prepared for each 310 OWs. For illustration, sample calculation of one OW (out of 310 OWs) is shown in Table 3. ME was estimated for each OW in the study area. The entropy values were estimated for all the years from 1999 to 2012. The uncertainty in each OW was analysed and the results were compared for January, March, May and October months. In order to compare the estimated results, ME values were OWs = OW, GWLs = GWL in m amsl, f = frequency normalised on a 0 to 100 scale [equation (3)], where ‘0’ indicates lowest uncertainty and 100 indicate the highest uncertainty. Table 4 shows the sample calculations for some OWs, where ME was converted to normalised marginal entropy (NME) and similar computations were performed for other OWs.

$$ME_n = \frac{ME - ME_{\min}}{ME_{\max} - ME_{\min}} \times 100 \tag{3}$$

where ME_n = NME (no unit), ME_{\max} = maximum values of ME (bits) and ME_{\min} = minimum values of ME (bits).

Table 3 Sample table for estimation of ME from year 1999 to 2012 for one OW (out of 310 OWs)

<i>GWLs</i>	<i>f</i>	<i>p(X)</i>	$\log_2 p(X)$	$-p(X) \times \log_2 p(X)$
245–250	1	0.07	–3.81	0.27
250–255	1	0.07	–3.81	0.27
255–260	1	0.07	–3.81	0.27
260–265	3	0.21	–2.22	0.48
265–270	2	0.14	–2.81	0.40
270–275	4	0.29	–1.81	0.52
275–280	1	0.07	–3.81	0.27
280–285	1	0.07	–3.81	0.27
$\Sigma -p(X) \times \log_2 p(X) = 2.75$				

2.4 Optimisation of GWLMN

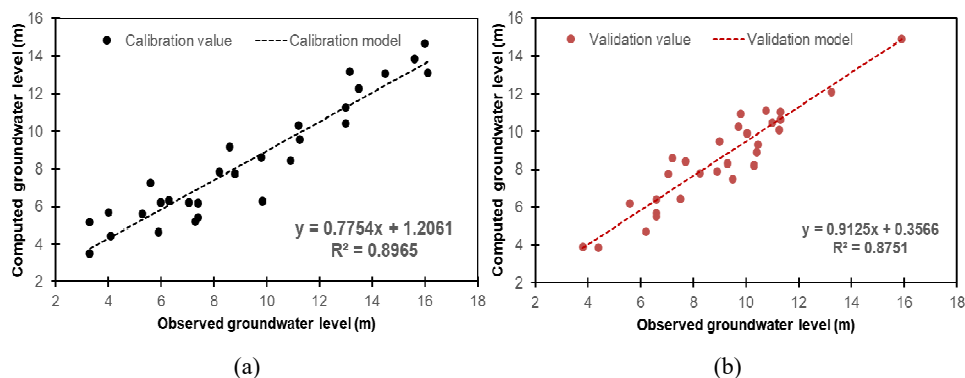
In the final step, the results obtained from groundwater flow and uncertainty analysis were utilised in conjunction with hydrological and anthropogenic parameters in a GIS environment to optimise the GWLMN. OWs were grouped based on uncertainty results, hydrological and anthropogenic parameters (Figure 1 and Table 1). The parameters associated with uncertainty in each OWs were analysed to obtain the optimal network. In this approach, uncertainty in each OW along with parameters such as land use/land cover (LU/LC), proximity to a water body, NCA, CA, aquifer properties, and existing OWs in the study, were utilised in a GIS environment to obtain the optimum monitoring network of OWs (Figure 1: steps 2 and 3). In each step, OWs with uncertainty values were added in each grid of size 3 km × 3.8 km. Based on the uncertainty results and scientific parameters, suitability to retain or remove OWs were examined and the grid was refined. Three thematic layers as grid, OWs, and proximity to water body were added together and based on the uncertainty and the associated properties of parameters, suitability to retain or remove the observation was examined for each OWs in a grid. For example,

OWs selected based on GWL uncertainty, i.e., ME and the yield ranges of aquifers (Tables 1 and 3). OWs removed or retained using two criteria:

- 1 OWs with low ME and high yield values were removed
- 2 OWs with high ME and low yield were retained and considered as significant for monitoring.

Consequently, the refined grid was further analysed and with three thematic GIS layers such as grid, refined OWs, and other parameters including aquifer properties, NCA and CA etc. and the step was repeated until all the assumed controlling parameters were satisfied. Land use/land cover of the study area was classified as agricultural land (rabi, kharif, and double/triple crop), non-agricultural land (built-up area, water bodies, and wastelands), and forest (NRSC, 2014).

Figure 4 Calibration and validation simulation plot of the study area, (a) calibration (1999–2005) (b) validation (2006–2012) (see online version for colours)



3 Results and discussion

3.1 Calibration and validation results of groundwater flow model

A steady-state groundwater flow model was achieved for the year 2011 pre-monsoon. Initially, a forward model was run to calibrate the model, but more time was required to converge the model. It was observed that the model was not easily converging, the study area being a complex aquifer system (Figure 1 and Table 1). Subsequently, an inverse modelling approach was adopted to calibrate the complex aquifer properties. For the inverse modelling, a calibration target of 1 m head was fixed. An iterative procedure was adopted to adjust the model parameters until the model computed values matching the field observed values to an acceptable level of calibration target (less than or equal to 1 m). The inverse model was run to keep hydraulic conductivity as a variable and the other parameters as constants. The calibration period was from 1999 to 2005, while the validation period was from 2006 to 2012 (Figure 4).

The results of observed and computed GWLs obtained from the inverse modelling are represented in Figure 5. It was observed that the calibration target was achieved and the difference between the observed and computed values is less [Figures 5(b) and 5(c)].

Table 4 Relationship between ME and NME for selected OWs

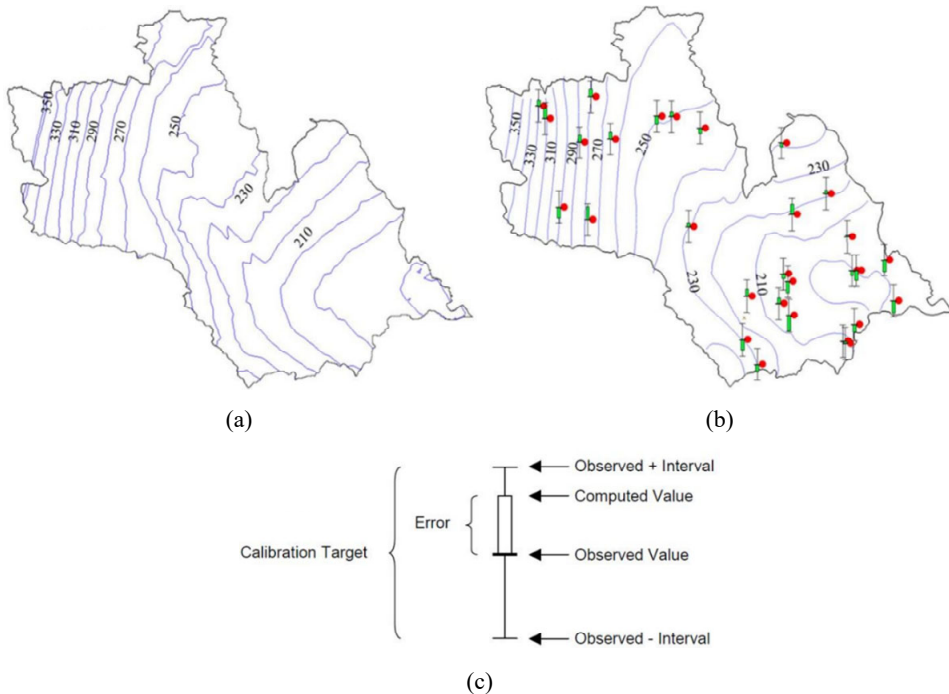
OW	219		231		308		277		127		10	
	GWLS	f	GWLS	f	GWLS	f	GWLS	f	GWLS	f	GWLS	f
	245-250	14	275-280	2	250-255	1	335-340	1	360-365	3	245-250	1
			280-285	12	255-260	10	340-345	2	365-370	2	250-255	1
					260-265	3	345-350	5	370-375	6	255-260	1
							350-355	6	375-380	3	260-265	3
											265-270	2
											270-275	4
											275-280	1
											280-285	1
Total $\sum f$		14		14		14		14		14		14
ME		0.0		0.59		1.09		1.73		2.21		2.75
NME		0		20		40		60		80		100

Notes: OWs = observation wells, GWLS = groundwater level in m amsl, f = frequency, NME = normalised marginal entropy.

3.2 Season wise uncertainty results in each hypothetical OW

The groundwater head contours obtained from the flow model were exported in the grid format. Hypothetical OWs were added to each grid (Figure 6). A total of 310 hypothetical OWs were considered for uncertainty analysis. The magnitude of GWLs in each OW was equal to the groundwater head obtained from groundwater flow modelling. The uncertainty in the each OW was observed for the months of January, March, May and October during 1999 to 2012. The entropy values range from 0 to 100 where ‘0’ indicates lowest uncertainty and 100 indicate highest uncertainty.

Figure 5 Groundwater head contour in m amsl for, (a) observed values (b) computed values (c) calibration target (see online version for colours)



Based on the uncertainty analysis results, NME values such as 0–20, 21–40, 41–60, 61–80 and 81–100 were grouped into very low, low, moderate, high, and very high uncertainty (Figure 7). The results of the entropy analyses show that the location of hypothetical OWs present in the months of March and May were the most uncertain. Low uncertainty values in OW indicate that the GWL measurement is more predictable. On the other hand, if high uncertainty prevails, then GWL measurement fluctuates more over a period of time.

Hence uncertainty is one of the criteria utilised in this study to assure the suitability of OWs for GWL measurement. If OWs have low uncertainty, then OWs can be removed from the monitoring network. On the contrary, if OWs have high uncertainty, then OWs can be retained. But, the judgement only based on uncertainty analysis will provide biased results (Singh and Katpatal, 2017a). In addition to uncertainty values of OWs,

there are several other hydrological and anthropogenic parameters which influence changes in GWL.

Figure 6 Hypothetical and existing OWs in each grid within the study area (see online version for colours)

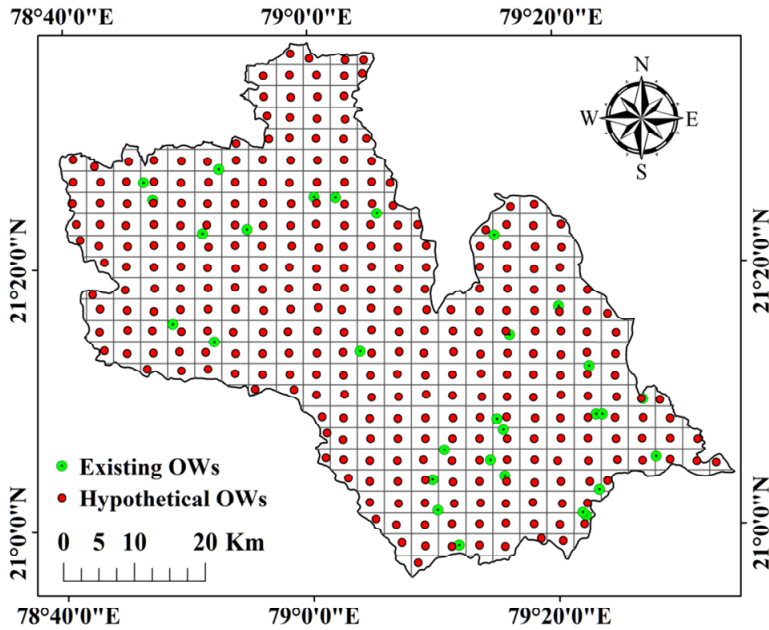
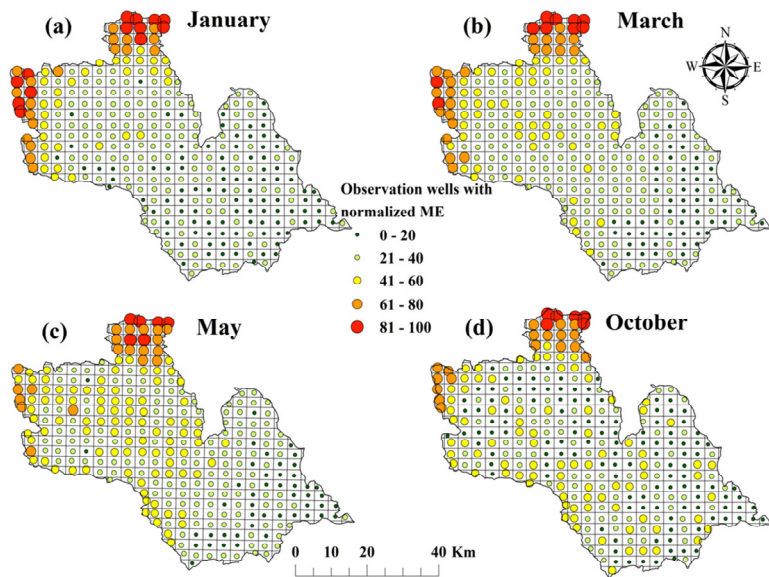


Figure 7 NME map of January, March, May and October from year 1999 to 2012 (see online version for colours)



3.3 *Aquifer wise results of uncertainty in existing OW*

Six complex aquifer systems in the study area are alluvium, amgaon gneissic complex, mica schist, basalt, calc gneiss marble and unclassified gneissic complex. The aquifer properties play an important role in the distribution and movement of groundwater, therefore the variation between aquifer systems of the study area affects the changes in GWLs. The aquifer properties in the study area were briefly described in Table 1 and Figure 1. The ME was estimated in each OW for each of the different aquifer systems. The results show that ME of the OWs varies between 0 to 100 (Figure 8). The high and low uncertainty values were observed in the OWs for different aquifer system. Overall, high ME values were observed in amgaon gneissic complex followed by basalt, unclassified gneissic complex, amgaon gneissic complex, mica schist, and alluvium. It was observed that the result obtained from the uncertainty analysis harmonises well with yield values of the aquifers. For example, high uncertainty values were reported in the OWs present in low yield aquifers such as amgaon gneissic complex and basalt, whereas, low uncertainty values found in the OWs having high yield aquifers of the alluvium aquifer system.

3.4 *Optimisation of GWLMN*

Optimisation of GWLMN was done using uncertainty analysis in conjunction with the hydrological and anthropogenic parameters in a GIS environment. The subsequent section shows the optimisation results by considering hydrological and anthropogenic parameters such as water body, LU/LC, NCA, CA, aquifer properties and existing OWs were utilised to optimise the GWLMN. Based on the uncertainty results and individual scientific parameters (Chandan and Yashwant, 2017), suitability to retain or remove OWs were examined and the grid was refined for redesign using GIS.

3.4.1 *Water body*

First, the water body and uncertainty results of OWs in each grid were superimposed. The presence of surface water body near the OWs has direct influence on the GWL measurement (Singh and Katpatal, 2017b). Hence, OWs were removed based on uncertainty results and the presence of water bodies [Figure 9(a)]. OWs present in each grid were refined and OWs in the GWLMN were removed, based on the combination of uncertainty results and the presence of water body in each grid. Total 78 OWs were found within the proximity of the water bodies, and hence they were removed [Figure 9(b)]. Thus, out of 310 OWs, 232 OWs were remaining in the GWLMN.

3.4.2 *Land use/land cover, CA, and NCA*

Land use classification in the study area consists of agricultural land, built up, water bodies and non agricultural land (forest and barren land) (Figure 10). Depending upon the crop water requirements, the study area was further classified into the CA and NCA. In NCA, the major source of water for irrigation is groundwater while in CA, surface water is the major source. The OW network was further refined based on uncertainty results and the LU/LC characteristics of the study area. The OWs network obtained from the result of the previous section with 232 OWs (proximity to water body) was input for this

analysis. Groundwater use is less in the forest area, non agricultural land, and CA. The OWs present in non agricultural land, CA and forest areas with low uncertainty were removed from the network of 232 OWs. Based on the results of this analysis, 112 OWs were further removed from the network of 232 OWs.

Figure 8 Uncertainty assessment of the existing OWs in the study area for different aquifer types (see online version for colours)

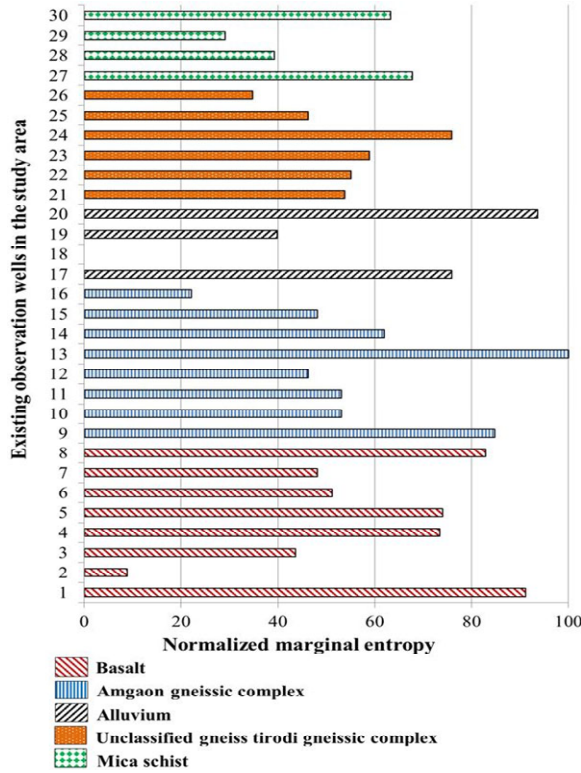


Figure 9 (a) OWs (310) with NME and water body (b) Optimised OWs (232) after considering uncertainty and water body (see online version for colours)

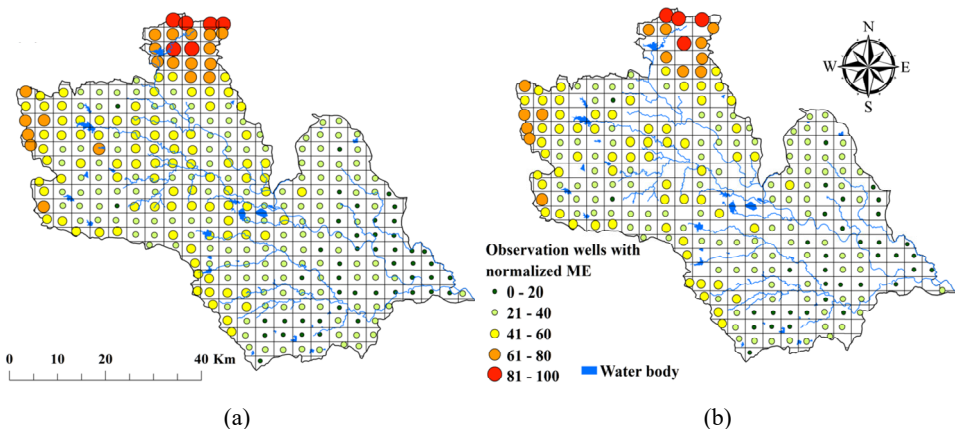
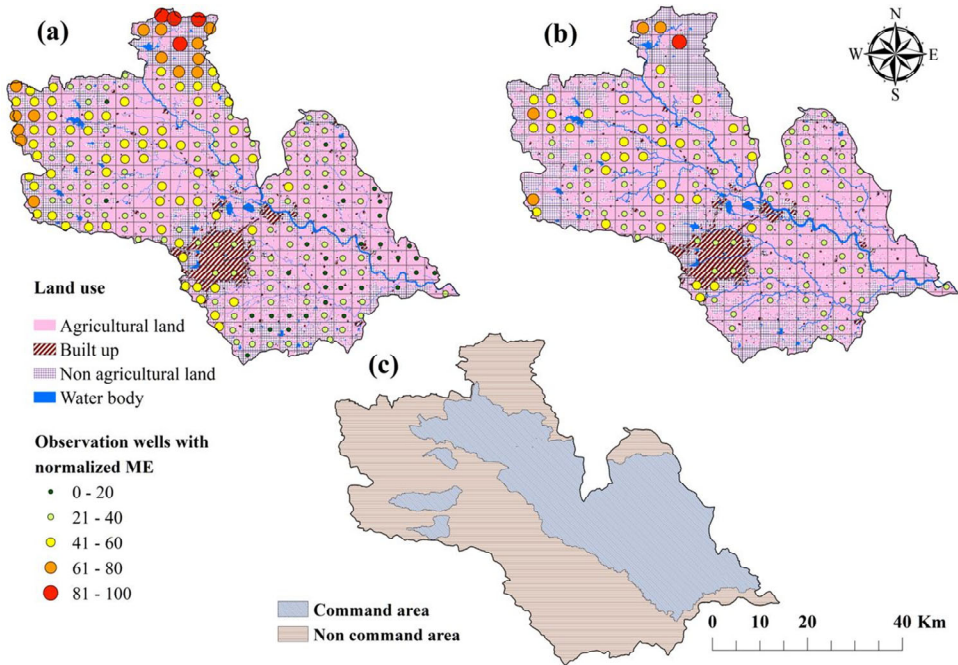


Figure 10 (a) OWs (232) with NME (b) Optimised OWs after considering (120) after considering uncertainty and LULC (see online version for colours)



3.4.3 Aquifer properties

The availability of groundwater resources in the aquifer is directly governed by the hydrological properties of the aquifer (Singh and Katpatal, 2017b). The lowest yield values were reported for amgaon gneissic complex, followed by the unclassified gneissic complex, mica schist, calc gneiss marble, and basalt. High yield values were observed for alluvium (Table 1). High uncertainty values were found in low yielding aquifers, whereas, low uncertainty values were found in the OWs in the alluvium (Figure 7 and Table 1). The OWs network was further refined on the basis of uncertainty results and complex aquifer properties (Table 1). The input of 120 OWs network was obtained from the result of the previous section (LU/LC, CA, and NCA). The OWs located in alluvium with low uncertainty values were removed from the network of 120 OWs [Figure 11(a)]. Based on the results obtained from this analysis, 10 more OWs were removed from the network of 120 OWs [Figure 11(b)].

The number of OWs located in the grid was refined based on the combination of uncertainty results, hydrological and anthropogenic parameters. Optimised network redesigned by further refining by comparing the spatial location of hypothetically assigned and existing OWs network (Figure 12). The overlapping common regions where the grids were assigned both the hypothetical OWs and existing OWs were identified. With the input of 110 OWs (hypothetical) and 29 existing OWs, 23 OWs (hypothetical) were removed from the grid. Hence, finally at the end of this analysis 116 OWs were identified as the preferred location of OWs.

Figure 11 (a) OWs (120) with NME (b) Optimised OWs (110) after considering uncertainty and aquifer properties (see online version for colours)

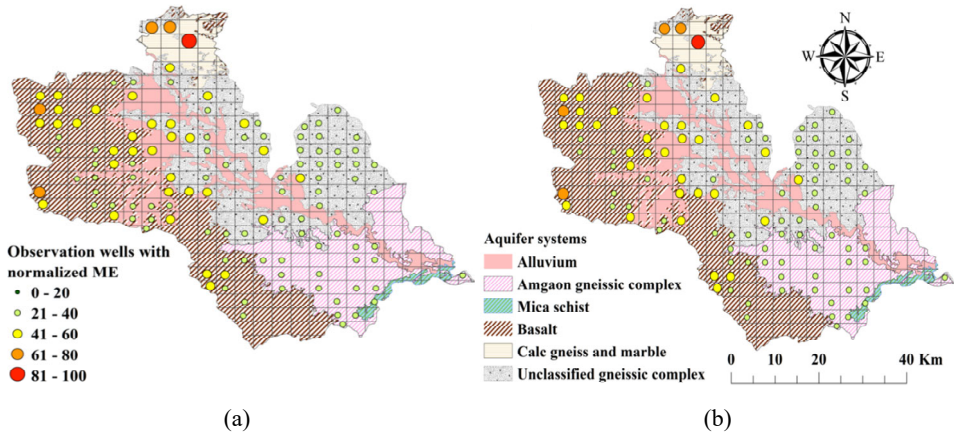
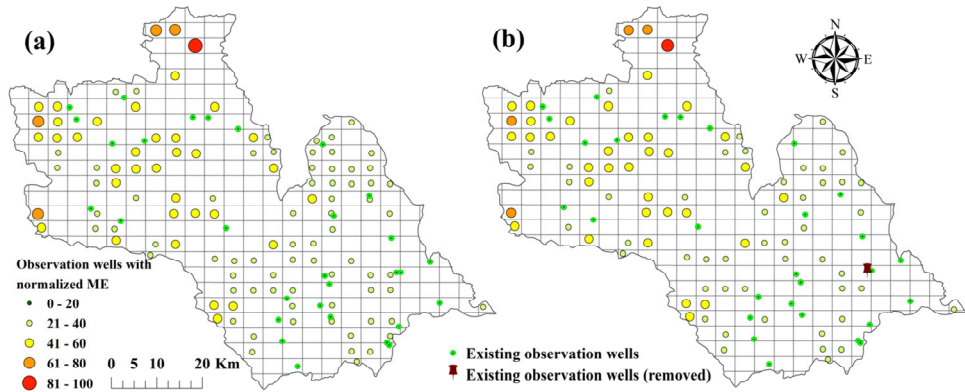


Figure 12 (a) Optimised OWs (110) after considering hydrological and anthropogenic parameters (b) Final optimised GWLMN (116 OWs) with 87 hypothetical OWs and 29 existing OWs (see online version for colours)



This study underlines the utility of GIS, groundwater flow modelling and entropy theory to optimise the GWLMN. The finding of the study includes statistical results (entropy) as well as scientific parameters for effective design of the monitoring network. This study further widens the existing knowledge of optimisation of the groundwater monitoring network. The proposed method shows clear advantage over other optimisation methods appeared in recent research. For example, Mondal and Singh (2012) have employed information of existing OWs for optimisation of the network in the Kodanagar River Basin, but it does not confirm anything where there are no OWs.

Hosseini and Kerachian (2017) designed the network using data fusion-based methodology, but, no controlling parameters were considered during the design. These approaches had not considered important multiple parameters to support the design results. From the previous study, it may be observed that the entropy theory is applicable for assessment and redesign of monitoring network using only existing network of OWs.

However, to overcome this drawback, the present study suggests a new methodology to assess and redesign GWLMN.

4 Conclusions

The GWLMN was assessed and redesigned by using a groundwater flow model and entropy theory in a GIS environment. The study was performed in the complex aquifer system of the Wainganga Basin, Central India from years 1999 to 2012. The groundwater flow model was calibrated and validated using the MODFLOW. Uncertainty in existing and hypothetical OWs was estimated using entropy or information theory. These uncertainties were analysed in each hypothetical OWs for January, March, May and October months. The results were analysed in space and time for 1999 to 2012. The results of the study show that a minimum of 116 OWs were significant for effective GWL monitoring. The study suggests that the inclusion of hydrological and anthropogenic parameters at the time of design, can significantly improve a GWLMN. Inclusion of GW flow model confirms that discrete (entropy)-based analysis and design can be applied for spatial and temporal domain. Groundwater flow modelling (GWFM) provides spatially explicit GWLs. Uncertainty analysis improved in optimising the spatially distributed parameters. GIS incorporates both the spatial-temporal accuracy and different hydrological and anthropogenic parameters. The study also suggests that the present method can be further refined and applied to design hydrometric networks such as precipitation, stream flow and groundwater quality networks.

References

- Ansari, T.A., Katpatal, Y.B. and Vasudeo, A.D. (2016) 'Integrated approach of geospatial visualization and modeling for groundwater management in hard rock terrains in Nagpur Urban Area, India', *Arabian Journal of Geosciences*, Vol. 9, No. 4, p.325.
- CGWB (2012) *Principal Aquifer System and Their Properties in Nagpur District* [online] <http://www.india-wris.nrsc.gov.in/LithologApp.html?UType=R2VuZXJhbA==?UName=> (accessed 13 on October 2016).
- CGWB (2014) *Assessment of Ground Water Resources: A Review of International Practices* [online] <http://www.cgwb.gov.in/GWAssessment/Review%20of%20International%20Practices%20on%20Assessment%20of%20GW%20Resources.pdf> (accessed 1 April 2017).
- Chandan, K.S. and Yashwant, B.K. (2017) 'Optimization of groundwater level monitoring network using GIS-based geostatistical method and multi-parameter analysis: a case study in Wainganga Sub-Basin, India', *Chinese Geographical Science*, Vol. 27, No. 2, pp.201–215.
- CWC and NRSC (2014) *Dams in Godavari Basin* [online] <http://www.india-wris.nrsc.gov.in> (accessed 14 June 2016).
- Davis, J.C. (2002) *Statistics and Data Analysis in Geology*, John Wiley & Sons, New York.
- GSI (2009) *Briefing Book, Report on Thematic Mapping of Deccan Traps in Inter-operational Areas Falling in Parts of Amravati and Nagpur Districts of Maharashtra, Chhindwara and Betul Districts of Madhya Pradesh*, Geological Survey of India [online] <https://www.gsi.gov.in/webcenter/portal/OCBIS> (accessed 27 October 2015).
- Hosseini, M. and Kerachian, R. (2017) 'A data fusion-based methodology for optimal redesign of groundwater monitoring networks', *Journal of Hydrology*, Vol. 552, pp.267–282.

- Júnez-Ferreira, H.E. and Herrera, G.S. (2013) 'A geostatistical methodology for the optimal design of space-time hydraulic head monitoring networks and its application to the Valle de Querétaro aquifer', *Environmental Monitoring and Assessment*, Vol. 185, No. 4, pp.3527–3549.
- Katpatal, Y.B., Pophare, A.M. and Lamsoge, B.R. (2014) 'A groundwater flow model for overexploited basaltic aquifer and Bazada formation in India', *Environmental Earth Sciences*, Vol. 72, No. 11, pp.4413–4425.
- Kelly, B.F.J., Timms, W.A., Andersen, M.S., McCallum, A.M., Blakers, R.S., Smith, R., Rau, G.C. et al. (2013) 'Aquifer heterogeneity and response time: the challenge for groundwater management', *Crop and Pasture Science*, Vol. 64 No. 12, pp.1141–1154, CSIRO Publishing.
- Li, C., Singh, V.P. and Mishra, A.K. (2012) 'Entropy theory-based criterion for hydrometric network evaluation and design: maximum information minimum redundancy', *Water Resources Research*, Vol. 48, No. 5 [online] <https://doi.org/10.1029/2011WR011251>.
- Manzar, A. (2013) *Ground Water Information Nagpur District Maharashtra*, pp.1–21, 1770/DBR/2013 [online] http://cgwb.gov.in/District_Profile/Maharashtra/Nagpur.pdf (accessed 23 September 2016).
- Mishra, A.K. and Coulibaly, P. (2009) 'Developments in hydrometric network design: a review', *Reviews of Geophysics*, Vol. 47, No. 2 [online] <https://doi.org/10.1029/2007RG000243>.
- Mondal, N., Singh, V. and Sankaran, S. (2011) 'Groundwater flow model for a tannery belt in Southern India', *Journal of Water Resource and Protection*, Vol. 3 [online] <https://doi.org/10.4236/jwarp.2011.32010>.
- Mondal, N.C. and Singh, V.P. (2012) 'Evaluation of groundwater monitoring network of Kodaganar River Basin from Southern India using entropy', *Environmental Earth Sciences*, Vol. 66, No. 4, pp.1183–1193.
- NRSC (2014) *Land Use/Land Cover Database on 1:50,000 Scale*, Natural Resources Census Project, LUCMD, LRUMG, RSAA, National Remote Sensing Centre, ISRO, Hyderabad [online] <http://bhuvan.nrsc.gov.in/gis/thematic/index.php> (accessed 21 September 2016).
- Ritzi, R.W. and Soltanian, M.R. (2015) 'What have we learned from deterministic geostatistics at highly resolved field sites, as relevant to mass transport processes in sedimentary aquifers?', *Journal of Hydrology*, Vol. 531, pp.31–39.
- Samuel, J., Coulibaly, P. and Kollat, J. (2013) 'CRDEMO: combined regionalization and dual entropy-multiobjective optimization for hydrometric network design', *Water Resources Research*, Vol. 49, No. 12, pp.8070–8089.
- Shannon, C.E. and Weaver, W. (1949) *The Mathematical Theory of Communication*, Univ. of Illinois Press, Urbana, IL.
- Shigidi, A. and Garcia, L.A. (2003) 'Parameter estimation in groundwater hydrology using artificial neural networks', *Journal of Computing in Civil Engineering*, Vol. 17, No. 4, pp.281–289, American Society of Civil Engineers.
- Singh, C.K. and Katpatal, Y.B. (2017a) 'Evaluating control of various hydrological factors on selection of groundwater-level monitoring networks in irrigated areas using a geospatial approach', *Journal of Irrigation and Drainage Engineering*, Vol. 143, No. 8, p.5017003, American Society of Civil Engineers.
- Singh, C.K. and Katpatal, Y.B. (2017b) 'A GIS based design of groundwater level monitoring network using multi-criteria analysis and geostatistical method', *Water Resources Management*, Vol. 31, No. 13, pp.4149–4163.
- Singh, C.K. and Katpatal, Y. (2020a) 'A review of the historical background, needs, design approaches and future challenges in groundwater level monitoring networks', *Journal of Engineering Science and Technology Review*, Vol. 13, No. 2, pp.135–153.
- Singh, C.K. and Katpatal, Y.B. (2020b) 'Assessment of groundwater-level monitoring network in irrigated regions with a complex aquifer system using information theory', *Journal of Hydrologic Engineering*, Vol. 25, No. 11, p.5020040.

- Todd, D.K. and Mays, L.W. (1980) *Groundwater Hydrology*, 3rd ed., John Wiley & Sons, New York, USA.
- Varalakshmi, V., Venkateswara Rao, B., SuriNaidu, L. and Tejaswini, M. (2014) 'Groundwater flow modeling of a hard rock aquifer: case study', *Journal of Hydrologic Engineering*, Vol. 19, No. 5, pp.877–886, American Society of Civil Engineers.
- Wang, K., Guan, Q., Chen, N., Tong, D., Hu, C., Peng, Y., Dong, X. et al. (2017) 'Optimizing the configuration of precipitation stations in a space-ground integrated sensor network based on spatial-temporal coverage maximization', *Journal of Hydrology*, Vol. 548, pp.625–640.